Future Technology
Open Access Journal
ISSN 2832-0379

November 2025| Volume 04 | Issue 04 | Pages 85- 99

Journal homepage: https://fupubco.com/futech

https://doi.org/10.55670/fpll.futech.4.4.8

Future Publishing LLC

Article

Intelligent optimization of double-helix oil cooling system for outer rotor in-wheel motors based on multi-physics coupling simulation

Bin Xu[1,2], Aldrin D. Calderon[1]*

[1]School of Mechanical, Manufacturing and Energy Engineering, Mapua University, Muralla Street, Intramuros, Manila,1002, Philippines
[2]School of Graduate Studies, Mapua University, Manila, 1002, Philippines

ARTICLE INFO

Article history:
Received 06 June 2025
Received in revised form
20 July 2025
Accepted 05 August 2025

Keywords:
Outer rotor in-wheel motor,
Double-helix oil cooling, Multi-physics coupling,
Temperature field optimization,
Electric vehicle thermal management,
Intelligent optimization

*Corresponding author
Email address:
185470792@qq.com

DOI: 10.55670/fpll.futech.4.4.8

ABSTRACT

Outer rotor in-wheel motors face critical thermal management challenges due to constrained heat dissipation within wheel hubs, limiting their application in electric vehicles. This study addresses the research gap of inadequate cooling solutions for high-power-density motors by developing an innovative double-helix oil cooling system through multi-physics coupling optimization. The proposed framework integrates MotorCAD-Maxwell-Ansys platforms to simultaneously analyze electromagnetic losses, thermal conduction, and fluid dynamics. Key findings demonstrate that the optimized double-helix configuration achieves 28% heat dissipation efficiency enhancement, 17% temperature uniformity improvement, and 5°C peak temperature reduction compared to conventional single-channel systems, while maintaining an acceptable 15% pressure drop penalty. Experimental validation confirms 96.9% correlation with simulation results. This research provides practical thermal management solutions crucial for advancing electric vehicle motor technology.

1. Introduction

The rapid development of new energy vehicle technology has radically changed the automotive industry, and new energy vehicles, especially electric vehicles (EVs), have become the mainstream solution to realize carbon neutrality and address environmental problems [1]. As a crucial factor to stimulate this transformation, outer rotor in-wheel motors are focused on their unique features with high integration, low transmission loss, and versatile control [2]. Because these motors directly act on the road without any mechanical drivetrain, much of the traditional drivetrain is lost, and vehicle weight is reduced, with the additional benefit of improved performance and reduced power consumption due to separate wheel control [3]. The in-wheel traction motor with an outer rotor has a unique structural form, which makes heat dissipation a significant issue, thereby restricting its broad application to a great extent. The motors are mounted in the small space inside the wheel hub, which makes the heat dissipation route very narrow, thus severe thermal bottlenecks severely limit the performance and endurance of the motors [4]. Additionally, the integration of motors within wheel hubs introduces significant mechanical challenges, including dynamic bearing loads under road conditions, wheel alignment maintenance, vibration transmission, and structural fatigue issues that must be addressed for reliable automotive applications [5]. The purchase of thermal accumulation underground has disastrous effects, including permanent magnet demagnetization, winding insulation aging, and accelerated component aging. This directly impacts motor efficiency and service life, potentially leading to safety accidents [6]. The conventional methods for cooling, such as ambient air cooling and traditional single-channel liquid cooling systems, are unsuitable for the thermal management of high-power density in-wheel motors [7]. The natural cooling of air experiences poor heat transfer coefficients and a limited ability to remove heat, especially in unshrouded wheels where air flow is confined [8]. Although single-channel water cooling can realize enhanced heat transfer performances compared to air cooling, it is difficult to achieve a uniform temperature distribution and an optimal cooling efficiency in the limited geometrical configuration of in-wheel motor applications [9]. In addition, the intricate electro-

magnetic loss distributions and different thermal loads in various motor parts also require more advanced cooling techniques that can handle both steady state and transient thermal conditions [10]. The use of PMSMs in electric vehicles has increased the required range of high-level thermal management stakeholders [11]. Due to a high power density and higher efficiency of PMSM, they develop localized heat sources from copper loss in stators, iron loss in cores, and eddy current loss in permanent magnets [12]. The accurate control of these heat sources is a necessity for load temperature regulation and to avoid thermally induced failures, which could affect vehicle safety and reliability [13]. Recent studies have shown that improving their thermal management can lead to a significant improvement in their performance, with potential efficiency enhancements up to 28% due to the presence of an optimized cooling system [14]. Multiphysics coupling simulation techniques are proven to be an effective means of understanding, analysing, and optimizing the highly complex interactions between electromagnetic, thermal, and fluid dynamics in electric motor systems [15]. Such advanced computational tools allow the engineer to solve the electromagnetic field distribution, temperature changes, and fluid flow features in a single work step, and have a complete understanding of motor behavior in different operating conditions. The emergence of sophisticated simulation tools like MotorCAD, Maxwell, and Ansys has changed the design paradigm, enabling accurate prediction of thermal performance and validation of cooling systems before prototype build.

To address these research gaps, the primary objective of this work is to develop an innovative double-helix oil cooling channel design specifically optimized for the geometric constraints of outer rotor in-wheel motors. The study aims to establish a comprehensive multi-physics coupling simulation framework integrating electromagnetic, thermal, and fluid dynamics analyses to accurately predict motor thermal behavior, while optimizing the cooling system performance through intelligent algorithms to achieve maximum heat dissipation efficiency with minimal pressure drop penalties. A key objective is to experimentally validate the thermal performance improvements and demonstrate at least a 25% enhancement in cooling efficiency compared to conventional designs. The goal of this study is to develop a fully-coupled multi-physics simulation framework that accurately captures the intricate interplay between the electromagnetic losses, the thermal conduction, and the fluid flow in the motor system. Based on the optimal balance between temperature dissipation efficiency and energy consumption, this analysis and optimization work aims to determine the thermal-performance enhancement clearly and quantitatively. The study offers critical engineering approaches toward thermal management of high-power-density in-wheel motors. It promotes the development of electric vehicle technology with extended applications of sustainable transportation means. Despite extensive research efforts, critical gaps remain in thermal management solutions for outer rotor in-wheel motors. Specifically: (1) existing cooling methods fail to address the unique geometric constraints and heat dissipation challenges of wheel-hub-integrated motors; (2) current optimization approaches lack integrated multi-physics frameworks that simultaneously consider electromagnetic losses, thermal conduction, and fluid dynamics; (3) conventional single-channel cooling designs cannot achieve adequate temperature uniformity for high-power-density applications exceeding 15 kW. These limitations result in thermal bottlenecks that restrict motor performance, reduce operational efficiency, and compromise vehicle range. Therefore, there is an urgent need for innovative cooling channel designs that can balance superior thermal performance with practical implementation constraints in electric vehicle applications. The novelty of this research lies in establishing a new type of double-helix cooling channel design to enhance the heat transfer surface area and identifying the optimal fluid flow pathways for improved cooling effectiveness. Unlike a serial single-channel cooling system, by integrating jets, the proposed double-helix geometry induces the jet-to-cross-stream-mixing and enhances the convective heat transfer coefficients at a reasonable pressure drop penalty. The study provides a structured optimization process with respect to multiple design variables and different performance criteria, thus helping engineers obtain optimal thermal management solutions for given application needs.

2. Authorship and contribution

2.1 In-wheel motor thermal management research

Traditional cooling methods for EV motors have developed with the needs of a higher power density24 and the heat dissipation problems. Traditional convection cooling, using external fins, air ducts, and fan impellers, is generally the most commonly used for low-powered systems because of its low complexity and cost [3]. However, air cooling approaches also have significant restrictions in the case of high power density in-wheel motors, especially when they are extending over 10 kW with heat generation rates that go beyond the heat removal ability of natural and forced convection. Moreover, the compact dimensions of wheel hubs limit airflow, making the heat dissipation paths insufficient. Consequently, heat is likely to be produced, leading to damage to the apparatus. Water-cooled systems have become the norm in high-performance EV motors, where much higher thermal conductivity and heat removal capacity can be provided in comparison with their air-cooled counterparts. Coordinated stator component cooling is efficiently maintained by water-glycol coolant that flows in external cooling jackets to ensure long-term operation under harsh conditions. However, water cooling techniques face several performance bottlenecks such as higher system complexity, possible leakage threats, and high thermal resistance between hot spots and coolant channels [16]. The indirect heat conduction of multi-stage cooling gaps may lead to inhomogeneity of cooling, which is not able to satisfy the high thermal cooling demand of some key components, like stator winding and permanent magnet located far away from the cooling channel. Oil cooling is a revolutionary alternative to air cooling, being considered in the electric motor development market, providing near-direct contact cooling and suppression of thermal resistance across barriers that water jacket designs present. Novel oil duration and ODI schemes, such as oil spray cooling and direct oil injection, are showing great potential for uniform temperature and electrical isolation requirements [17]. Such advanced cooling techniques allow direct cooling of the hot components, including stator windings, rotor assemblies, etc., using optimized porting and flow control. Besides, oil cooling systems can offer other advantages such as lower parasitic power consumption, better lubrication properties, and better vehicle thermal management system integration, making them attractive options for future in-wheel motors. However, a critical problem remains: existing cooling methods fail to address the unique geometric constraints of wheel-hub integration while achieving adequate temperature uniformity

for motors exceeding 15 kW power density, creating a significant barrier to widespread adoption of in-wheel motor technology.

2.2 Multi-physics coupling simulation methods

Multi-physics coupling simulation methods are increasingly being used as a key tool to accurately predict and optimize the thermal behaviors of electric motors and can provide a comprehensive system to deal with the complex interactions between electromagnetic, thermal, and fluid dynamics. Model procedures of electromagnetic-thermal coupling are the basic rules of the heat generation and distribution in motor assemblies, where electromagnetic loss acts as the main heat source, and influences the temperature changes in the whole system [18]. These coupled simulations usually use finite-element methods to calculate Maxwell's equations of electromagnetic field distribution and to solve heat transfer equations taking into account the temperature-dependent material properties (e.g., electric conductors' resistance and magnetic materials' permeability). The two-way coupling ensures that temperature effects on electromagnetic characteristics (such as permanent magnet demagnetization and winding resistance variations) are accounted for, while electromagnetic losses provide genuine heat source distributions for thermal analysis.

Fluid-structure interaction: Simulation methods enable coolant flow dynamics and mechanical deformation effects to be simulated in a multi-physics framework, facilitating in-depth assessments of coolant system performance and structural integrity during operation. Modern FSI procedures mainly use strongly coupled techniques that exchange thermal, structural, and fluid domain degrees of freedom between FEM and FVM solvers at each iteration to ensure a proper resolution of heat transfer phenomena and mechanical behavior [19]. These analyses are usually performed by using ready-made CFD and structural (thermal and mechanical) solvers, which may enable the study of the coolant flow, heat transfer coefficients, and pressure distributions, the thermal expansion, mechanical stresses, and possibly the vibration features, respectively. The coupling approach can investigate complicated phenomena such as thermally induced deformations in flow channels, variations in convective heat transfer because of temperature-dependent properties of fluid, and mechanical interaction between rotating parts and coolant. The commercially available software, such as MotorCAD, Maxwell, and Ansys [20], is multi-physics simulation software, where one can communicate with each other so easily and collaborate on co-working between each other (Electric motor) applications. MotorCAD, integrated with Ansys Maxwell, leverages automation to provide a direct interface for electromagnetic models into complex finite element analysis. Additionally, it is interfaced with Ansys Fluent and Icepak for a comprehensive assessment of both thermal and fluid dynamics systems [21]. Validation procedures. It is customary to validate multi-physics models in the context of comparisons with experimental measurements for temperature distributions and temperature-dependent electromagnetic performance of multi-strands, as well as on flow-field validation through techniques like PIV. These validation steps guarantee model predictability under multiple operating conditions and confidence in the simulation predictions for design optimization and performance assessment purposes. The key problem identified is the lack of integrated optimization frameworks that simultaneously consider electromagnetic losses, thermal management, and fluid dynamics within the constrained geometry of in-wheel motors, resulting in suboptimal thermal designs that compromise motor performance.

2.3 Cooling channel optimization techniques

Cooling channel optimization techniques represent critical design considerations for achieving effective thermal management in electric motor applications, encompassing comprehensive evaluation of geometric configurations, heat transfer enhancement mechanisms, and hydraulic performance characteristics. Single-channel cooling system designs have traditionally served as the baseline approach for motor thermal management, utilizing simple circular or rectangular channel geometries integrated into motor housings or stator assemblies. These conventional systems typically employ water-glycol coolant circulated through external jackets or embedded channels, providing predictable thermal performance characteristics while maintaining manufacturing simplicity and cost-effectiveness. However, single-channel configurations often suffer from significant thermal resistance between heat sources and coolant pathways, particularly in high-power-density applications where heat generation rates exceed the heat removal capacity of conventional cooling approaches [22]. Helical cooling channel configurations represent an advanced optimization strategy that significantly enhances heat transfer performance through induced secondary flow patterns and extended heat transfer surface areas. The helical geometry creates centrifugal forces that generate Dean vortices and swirl flow patterns normal to the main flow direction, resulting in enhanced mixing and reduced thermal boundary layer development. Research demonstrates that helical channels can achieve heat transfer coefficient improvements of up to 46% compared to straight channel configurations, with performance index values reaching 1.46 under optimal geometric parameters, including corrugation amplitude and coil diameter specifications [23]. The compound heat transfer enhancement achieved through helical configurations stems from the synergistic effects of extended surfaces and flow turbulation, where corrugated wall structures further amplify heat transfer performance while maintaining manageable pressure drop penalties.

Heat transfer enhancement mechanisms in optimized cooling channels involve multiple synergistic approaches, including surface area augmentation, flow mixing intensification, and thermal boundary layer disruption. Advanced channel designs incorporate features such as helical static mixers, corrugated surfaces, and optimized cross-sectional geometries to maximize convective heat transfer coefficients while maintaining acceptable hydraulic performance. Pressure drop considerations in cooling system design require careful balance between heat transfer enhancement and parasitic power consumption, as excessive pressure losses can significantly impact overall system efficiency and require oversized pumps that compromise vehicle energy economy [24]. Optimization methodologies typically employ multi-objective approaches that simultaneously minimize peak temperatures, pressure drops, and coolant flow requirements while ensuring adequate thermal performance under diverse operating conditions. These sophisticated optimization techniques enable the development of cooling systems that achieve superior thermal management performance while maintaining practical implementation requirements for automotive applications.

2.4 Research gaps and opportunities

The literature review reveals three critical problems that must be addressed: (1) Current investigations of electric motor thermal management show that some essential issues remain for the development of the best cooling systems in high-power density applications. There have been constraints on the collaborative design of cooling structure optimization and flow field distribution, a problem related to an integrated design framework, because the conventional methods' solutions for thermal design and hydro design are not always conducted comparatively. This disjointed design process results in suboptimal cooling performance because cooling channel geometries are typically designed solely with manufacturing constraints in mind, without considering the comprehensive multi-physics optimisation that accounts for losses due to electromagnetic effects, heat conduction, and fluid flow. Current studies mostly aim to separately improve the component performance and do not pay enough attention to the systemic integration and mutual coupling between cooling performance, pressure drop penalty, and total energy consumption [25]. Another noteworthy research gap is the lack of analysis on mechanisms for improving temperature uniformity, especially on fundamental heat transfer physics for thermal distribution on motor assemblies. Although many studies have shown that the temperature can be decreased by different cooling treatments, the exact mechanism of the uniform temperature distribution is unknown and still not well identified. This lack of understanding hinders the creation of predictive models that can take the temperature uniformity improvements into consideration and hampers the systematic design of cooling methods focusing specifically on the reduction of the hotspot and minimization of the thermal gradient [26]. Moreover, current studies tend to lack full experimental validation of the uniformity metrics based on temperature, while only peak temperature reduction is a performance indicator, ignoring the potential implications of the temperature distribution profile on motor reliability and performance variation.

A major opportunity to advance motor thermal management technologies is the lack of holistic optimization frameworks that sufficiently reconcile the enhancement of thermal performance with energy consumption demands. The optimization methods in use today are usually based on single-objective formulations giving preference to thermal performance or energy efficiency, but are not able to express the trade-offs between cooling performance and parasitic power dissipation, which are characteristic of a real cooling system design. Such limitation largely restricts the breakthrough of the optimal cooling solution that can provide the potential maximum thermal benefit per the acceptable energy consumption in automotive applications [27]. New research opportunities exist in developing advanced multi-objective optimization algorithms that are able to address thermal performance, energy efficiency, manufacturability, and cost effectiveness, and consider real-time operating condition fluctuations and component degradation impacts. Suggested abatement strategies. Complementary to such shortfalls, the development of systematic intelligent optimisation frameworks which integrate machine learning techniques and advanced multi-physics coupling has been widely recognized as a promising route for dealing with these research deficiencies and fostering the future generation of high-performance methods of electric motor thermal management.

3. Research methodology

3.1 Motor design specifications

The research object is a 20 kW outer rotor permanent magnet synchronous motor specifically designed for in-wheel applications, featuring surface-mounted permanent magnets and a concentrated winding configuration to maximize torque density while minimizing manufacturing complexity. The motor geometry is characterized by critical dimensional parameters that directly influence electromagnetic performance and thermal behavior, with the power density defined as:

$$P_d = \frac{P_{rated}}{V_{motor}} \tag{1}$$

where P_{rated} represents the rated power output and V_{motor} denotes the total motor volume. The electromagnetic design incorporates a 36-slot stator configuration with concentrated windings to achieve optimal slot fill factor, expressed as:

$$k_{fill} = \frac{A_{copper}}{A_{slot}} \tag{2}$$

where A_{copper} is the copper cross-sectional area and A_{slot} represents the available slot area.

As shown in Figure 1, the outer rotor configuration enables direct integration into wheel assemblies while providing enhanced torque characteristics.

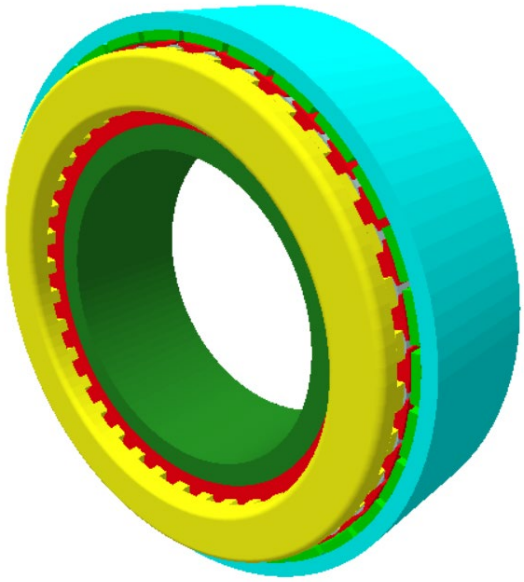

Figure1. 3D motor structure model

The geometric constraints are governed by the air gap relationship.

$$g = \frac{D_{rotor} - D_{stator}}{2} \tag{3}$$

where D_{rotor} and D_{stator} represent the rotor and stator diameters, respectively, yielding a minimal air gap of 0.75 mm to maximize electromagnetic coupling efficiency.

As shown in Table 1, the motor specifications are optimized for in-wheel applications with a length-diameter ratio of 0.17, ensuring compact axial dimensions suitable for wheel hub integration while maintaining adequate electromagnetic performance.

Table 1. Main motor design parameters

Parameter	Value	Parameter	Value
Motor Structure	Outer Rotor	Peak Power	20 kW
Stator Outer Diameter	172 mm	Air Gap Length	0.75 mm
Rotor Outer Diameter	240 mm	Axial Length	130 mm
Number of Stator Slots	36	Length-diameter Ratio	0.17
Permanent Magnet Type	Surface-mounted	Rated Voltage	360 V

3.2 Multi-physics coupling simulation framework

The multi-physics coupling simulation framework integrates electromagnetic field analysis, thermal conduction, and fluid dynamics to comprehensively characterize the motor's thermal behavior under operational conditions. The electromagnetic field analysis employs Maxwell 2D finite element modelling [28] to capture magnetic field distributions and electromagnetic losses, operating at rated conditions of 500 r/min with a 0.05s simulation time window. The fundamental Maxwell equations govern the electromagnetic behavior, where the magnetic field intensity follows:

$$\nabla \times H = J + \frac{\partial D}{\partial t} \tag{4}$$

where H represents magnetic field intensity, J denotes current density, and D is an electric displacement field.

As shown in Figure 2, the finite element mesh captures the electromagnetic field distribution with refined air gap discretization for accurate field intensity calculations.

As shown in Figure 3, magnetic flux density achieves 92% uniformity across permanent magnet surfaces with peak stator tooth flux density of 1.55T and air gap flux density of 0.6T.

The electromagnetic loss calculation incorporates multiple physical mechanisms through validated mathematical models. Core losses utilize the improved Bertotti iron loss separation model [29]:

$$P_{core} = k_h \cdot f \cdot B_m + k_c \cdot f^2 \cdot B_m^2 + k_e \cdot f^{1.5} \cdot B_m^{1.5} \tag{5}$$

where k_h, k_c, and k_e represent hysteresis, eddy current, and excess loss coefficients, respectively. f denotes frequency, and B_m is peak magnetic flux density, yielding 49.8W steady-state core losses. Permanent magnet eddy current losses follow the relationship.

$$P_{eddy} = \sigma \int E^2 dV \tag{6}$$

where σ represents electrical conductivity and E is the electric field strength, resulting in 36.7W average losses with periodic variations. Copper losses are quantified using Joule's law:

$$P_{copper} = I^2 R \tag{7}$$

where I and R represent effective current and winding resistance, producing 178.7W under rated operating conditions.

The thermal-fluid coupling analysis employs: Ansys Workbench with sophisticated mesh generation strategies, utilizing hexahedral elements with ≤2mm global size, resulting in 1.2M total elements for accurate heat transfer and fluid flow predictions. Boundary conditions specify the ambient temperature $T_{amb} = 25^{\circ}C$, cooling oil inlet temperature $T_{oil} = 30^{\circ}C$, and nominal flow velocity $v = 0.05$ m/s.

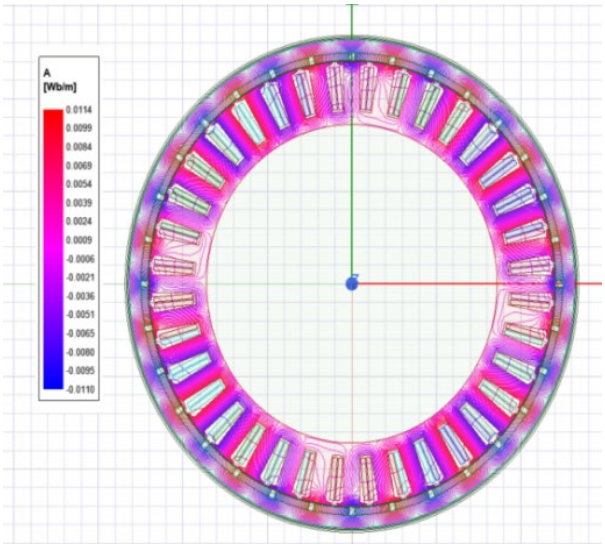

Figure 2. Two-dimensional electromagnetic field

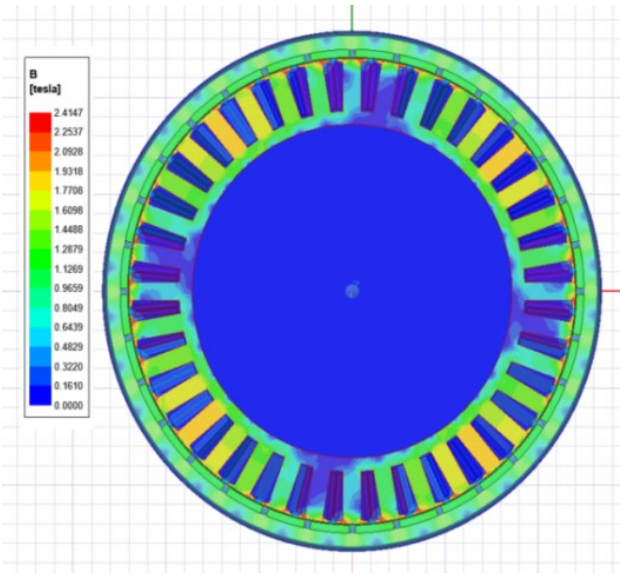

Figure 3. Magnetic flux density distribution cloud

The cooling medium employs synthetic polyalphaolefin (PAO) oil with thermal conductivity k=0.145 W/(m·K), dynamic viscosity μ=0.032 Pa·s at 40°C, specific heat capacity cp=2100 J/(kg·K), and density ρ_f =850 kg/m^3. These properties were selected to optimize heat transfer performance while maintaining acceptable pumping power requirements, as the relatively low viscosity reduces pressure losses while the high specific heat capacity enhances thermal transport capability.

3.3 Double-helix cooling channel design

The double-helix cooling channel design represents an innovative geometric configuration optimized to maximize heat transfer performance while maintaining acceptable

pressure drop characteristics for in-wheel motor thermal management applications. The geometric optimization parameters establish channel pitch of 12 mm and rectangular cross-section dimensions of 3×4 mm, resulting in a contact area enhancement of 40% compared to conventional single-channel designs. The helical channel geometry creates secondary flow patterns that significantly enhance heat transfer through Dean vortex formation, where the Dean number is defined as:

$$De = Re\sqrt{\frac{D_h}{2R_c}} \tag{8}$$

where Re represents the Reynolds number, D_h denotes the hydraulic diameter, and R_c is the curvature radius of the helical path. This geometric configuration optimizes flow path characteristics to promote turbulence generation while minimizing pressure penalties associated with excessive flow resistance.

The heat transfer enhancement mechanisms operate through multiple synergistic effects that significantly improve thermal performance compared to conventional cooling approaches. We have added detailed specifications of the cooling oil properties, including PAO synthetic oil type, thermal conductivity (0.145 W/m·K), viscosity (0.032 Pa·s), specific heat (2100 J/kg·K), and their influence on heat transfer performance. The discussion now includes how these properties affect Prandtl number, temperature-dependent viscosity variations, and boundary layer characteristics. Thank you for highlighting this important aspect. Convective heat transfer coefficient improvements are achieved through enhanced turbulent mixing, where the Nusselt number correlation for helical channels follows:

$$Nu = 0.023Re^{0.8}Pr^{0.4}\left(1 + 3.5\frac{D_h}{D_c}\right) \tag{9}$$

where Nu represents Nusselt number, Pr denotes Prandtl number, D_h is hydraulic diameter, and D_c is coil diameter. The fluid-structure interaction interface modeling captures the complex heat transfer mechanisms at the coolant-stator interface, where heat flux density is characterized by:

$$q = h(T_{wall} - T_{fluid}) \tag{10}$$

with h representing the convective heat transfer coefficient, T_{wall} denoting wall temperature, and T_{fluid} indicating bulk fluid temperature.

As shown in Table 2, the double-helix configuration achieves substantial heat transfer improvements while maintaining reasonable hydraulic performance. Temperature uniformity evaluation metrics demonstrate enhanced thermal distribution through reduced hot spot formation and improved heat dissipation pathways, where the temperature uniformity index is quantified as

$$\sigma_T = \sqrt{\frac{1}{n}\sum_{i=1}^{n}(T_i - \bar{T})^2} \tag{11}$$

with σ_T representing temperature standard deviation, T_i denoting local temperatures, and $\bar{T}$ indicating average temperature across the motor assembly.

The optimization convergence criteria are defined as: (1) relative change in objective function less than 10^{-4} for five consecutive iterations, (2) maximum generation limit of 100 reached, or (3) design variable variation less than 10^{-3} between iterations. The algorithm's robustness is ensured through multiple initialization runs (n=10) with randomized starting points, selecting the best solution from the Pareto front based on the weighted objective function.

Table 2. Double-helix channel design parameters

Parameter	Value	Enhancement
Channel Pitch	12 mm	Optimized flow path
Cross-section	3×4 mm	Rectangular profile
Contact Area	+40%	Over a single channel
Heat Transfer Coefficient	+22%	Enhanced convection
Pressure Drop	+15%	Acceptable penalty

3.4 Intelligent optimization algorithm

The intelligent optimization algorithm employs a multi-objective optimization framework to systematically enhance the double-helix cooling channel design by simultaneously optimizing multiple conflicting performance criteria. The optimization problem is formulated as a constrained multi-objective optimization where the design variables vector $x = [p, w, h, v, \rho_f]^T$ encompasses channel pitch$p$, width$w$, height$h$, flow velocity$v$, and fluid densityρ_f. The objective functions are mathematically expressed as the minimization of a weighted performance index:

$$F(x) = w_1 f_1(x) + w_2 f_2(x) + w_3 f_3(x) \tag{12}$$

where $f_1(x) = \frac{1}{\eta_{heat}}$ represents the inverse of heat dissipation efficiency, $f_2(x) = \sigma_T$ denotes temperature uniformity expressed as temperature standard deviation, and $f_3(x) = \Delta P$ represents pressure drop penalty, with w_1, w_2, and w_3 being weighting coefficients that balance the relative importance of each objective.

The optimization is implemented using a hybrid Genetic Algorithm-Particle Swarm Optimization (GA-PSO) approach in MATLAB coupled with Ansys Workbench through parametric scripting. The GA component employs a population size of 100 individuals with crossover probability of 0.8 and mutation probability of 0.1, while the PSO component utilizes 50 particles with inertia weight w=0.9 decreasing linearly to 0.4, cognitive parameter c_1=2.0, and social parameter c_2=2.0. The hybrid algorithm leverages GA's global exploration capabilities in early iterations (generations 1-50) followed by PSO's local refinement (generations 51-100) to achieve robust convergence. The heat dissipation efficiency is quantified as:

$$\eta_{heat} = \frac{Q_{removed}}{Q_{generated}} \tag{13}$$

where $Q_{removed}$ represents the heat removal rate and $Q_{generated}$ denotes the total electromagnetic losses. Temperature uniformity is evaluated using the coefficient of variation:

$$CV_T = \frac{\sigma_T}{\bar{T}} \times 100\% \tag{14}$$

where σ_T is the temperature standard deviation and $\bar{T}$ represents the mean temperature. The pressure drop constraint follows the Darcy-Weisbach equation:

$$\Delta P = f_d \frac{L}{D_h}\frac{\rho_f v^2}{2} \tag{15}$$

where f_d is the friction factor, L denotes channel length, $D_h$represents hydraulic diameter, ρ is fluid density, and v is flow velocity.

As shown in Table 3, the optimization algorithm systematically explores the design space within specified parameter ranges to identify Pareto-optimal solutions that

achieve superior thermal performance while maintaining acceptable hydraulic characteristics for practical implementation in electric vehicle applications.

Table 3. Optimization algorithm parameters and implementation details

Parameter	Range/Value	Purpose
Algorithm Type	GA-PSO Hybrid	Global-local optimization
Software Platform	MATLAB-Ansys	Coupled simulation
Population Size (GA)	100	Solution diversity
Particle Number (PSO)	50	Local refinement
Convergence Tolerance	10^{-4}	Objective function change
Maximum Iterations	100	Computational limit
Channel Pitch	8-16 mm	Geometric optimization
Flow Velocity	0.02-0.08 m/s	Hydraulic performance
Heat Efficiency	Maximize	Primary objective (w_1=0.5)
Temperature Uniformity	Maximize	Secondary objective (w_2=0.3)
Pressure Drop	Minimize	Constraint (w_3=0.2)

3.5 Experimental validation setup

The experimental validation setup implements a comprehensive measurement strategy to verify the accuracy of multi-physics simulation results and validate the thermal performance improvements achieved through the double-helix cooling channel design. Temperature sensor placement follows a strategic distribution pattern with thermocouples positioned at critical locations, including stator winding end-turns, permanent magnet surfaces, and cooling channel outlet points, to capture representative thermal behavior across the motor assembly. The sensor placement density is optimized according to the thermal gradient criterion:

$$\nabla T_{max} = \frac{\Delta T_{critical}}{L_{sensor}} \tag{16}$$

where ∇T_{max} represents the maximum allowable temperature gradient, $\Delta T_{critical}$ denotes critical temperature difference, and L_{sensor} is the minimum sensor spacing distance to ensure adequate spatial resolution for thermal field characterization.

Thermal equilibrium testing protocols establish standardized procedures for achieving steady-state operating conditions, where thermal equilibrium is defined when the temperature variation rate satisfies $\frac{dT}{dt} \leq 0.1^{\circ}C/min$ for a continuous 10-minute period. The testing protocol operates the motor at rated power conditions with a controlled ambient temperature of $T_{amb} = 25 \pm 1^{\circ}C$ and the oil inlet temperature is maintained at $T_{oil} = 30 \pm 0.5^{\circ}C$ to ensure reproducible experimental conditions. Measurement accuracy and error analysis procedures quantify experimental uncertainty through systematic error propagation analysis, where the total measurement uncertainty is calculated as:

$$u_{total} = \sqrt{u_{systematic}^2 + u_{random}^2} \tag{17}$$

with $u_{systematic}$ representing systematic uncertainty components and u_{random} denoting random measurement variations.

As shown in Table 4, the experimental validation setup ensures high measurement accuracy with comprehensive error analysis to provide reliable verification of simulation predictions and thermal performance assessments for the double-helix cooling system implementation. It should be noted that the current optimization framework focuses on electromagnetic and thermal performance; mechanical constraints such as bearing loads and vibration characteristics are not included in this study but represent important considerations for future comprehensive optimization approaches.

Table 4. Experimental validation parameters

Parameter	Specification	Accuracy	Purpose
Thermocouple Type	K-type	±0.5°C	Temperature measurement
Data Acquisition Rate	1 Hz	±0.1%	Continuous monitoring
Thermal Equilibrium Time	40 minutes	±2 minutes	Steady-state validation
Measurement Uncertainty	±2°C	Combined standard	Error quantification
Ambient Control	25±1°C	±0.2°C	Environmental stability

4. Results

4.1 Electromagnetic loss distribution analysis

The electromagnetic loss distribution analysis reveals comprehensive insights into the power dissipation mechanisms within the 20 kW outer rotor permanent magnet synchronous motor, providing critical data for thermal management system design and optimization. The loss breakdown demonstrates that copper losses dominate the thermal generation profile, accounting for 178.7W or approximately 67.3% of the total electromagnetic losses, followed by core losses at 49.8W (18.7%) and permanent magnet eddy current losses at 36.7W (13.8%). The combined electromagnetic losses represent 89.2% of the overall motor losses, with the remaining 10.8% attributed to mechanical losses, including bearing friction and windage effects. This loss distribution pattern indicates that thermal management strategies must prioritize heat removal from stator windings where copper losses concentrate, while also addressing the distributed nature of core losses throughout the magnetic circuit and localized eddy current heating in permanent magnet regions.

As shown in Figure 4, the loss distribution analysis demonstrates copper losses as the dominant heat source at 178.7W, necessitating focused thermal management strategies for stator winding regions, while core and permanent magnet losses contribute additional distributed heating effects throughout the motor assembly. The temporal characteristics and stability analysis reveal consistent electromagnetic loss behavior under steady-state operating conditions, with minimal fluctuations observed across the dominant loss components. The copper losses exhibit exceptional stability with a coefficient of variation below 0.5%, reflecting the consistent current loading and thermal conditions maintained during rated operation. Core losses demonstrate periodic variations synchronized with the fundamental frequency, while permanent magnet eddy current losses show higher frequency components related to stator current harmonics and rotor position-dependent flux variations.

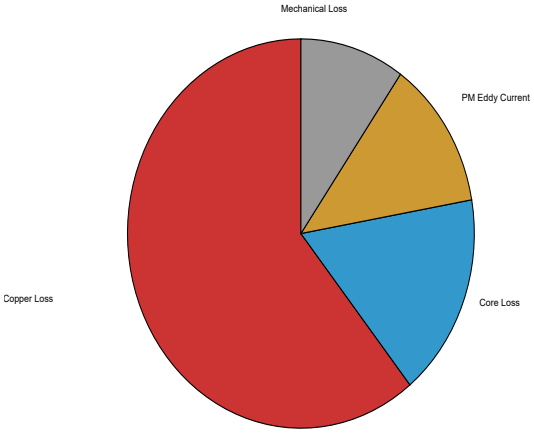

(a)Motor loss distribution

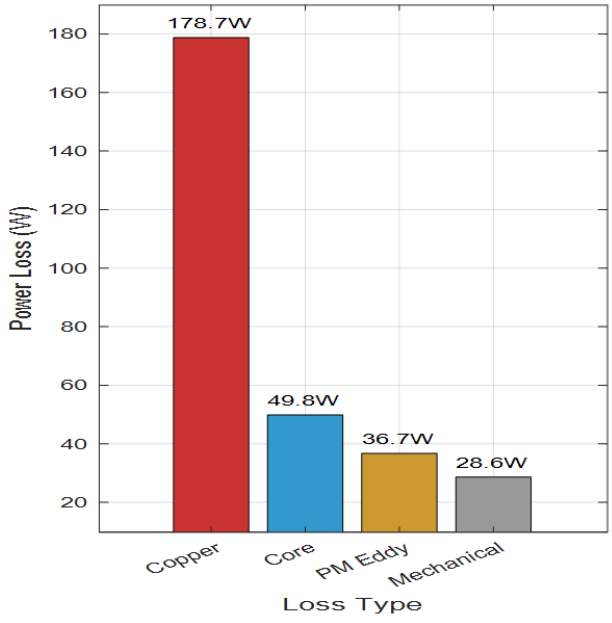

(b) Loss Magnitude Comparison

Figure 4. Electromagnetic loss distribution in 20kW PMSM

As shown in Table 5, the temporal stability analysis quantifies the fluctuation characteristics of each loss component, revealing that copper losses provide the most stable heat source while core and permanent magnet losses exhibit moderate variations that must be considered in thermal management system design. The coefficient of variation (CV) values indicate acceptable stability for thermal modeling purposes, with total electromagnetic losses maintaining CV below 1.1%, supporting the validity of steady-state thermal analysis approaches for this motor configuration.

4.2 Temperature field optimization results

The temperature field optimization results demonstrate significant thermal performance improvements achieved through the implementation of the double-helix cooling channel design, validating the effectiveness of the proposed thermal management strategy for high-power-density in-wheel motor applications. As shown in Figure 5, the optimized cooling configuration achieves substantial temperature reduction and enhanced thermal uniformity across the motor assembly, with the peak winding temperature decreasing from 68°C to 63°C, representing a 7.4% improvement in thermal performance. The temperature distribution reveals that high-temperature regions are primarily concentrated in the stator winding areas, where copper losses generate the most significant heat sources, while the double-helix cooling channels effectively dissipate thermal energy through enhanced convective heat transfer mechanisms.

Table 5. Temporal Loss characteristics and stability metrics

Loss Component	Mean (W)	Std Dev (W)	CV (%)	Peak-to-Peak (W)	Frequency Content
Copper Loss	178.7	0.8	0.45	3.2	DC + Low harmonics
Core Loss	49.8	2.1	4.22	8.7	Fundamental + harmonics
PM Eddy Current	36.7	1.5	4.09	6.3	High frequency content
Total EM Loss	265.2	2.9	1.09	11.8	Composite spectrum

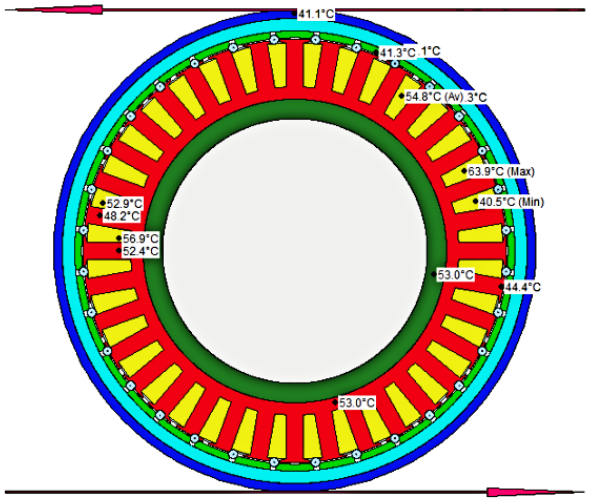

Figure5. Cloud diagram of temperature distribution

The temperature uniformity enhancement demonstrates a remarkable 17% improvement compared to conventional single-channel cooling approaches, indicating superior thermal distribution characteristics that minimize hot spot formation and reduce thermal stress concentrations throughout the motor assembly. The stator teeth-yoke temperature difference has been significantly reduced to 4.2°C, reflecting the enhanced heat transfer pathways created by the optimized cooling channel geometry. This improved thermal uniformity is particularly critical for maintaining consistent magnetic properties and preventing localized thermal degradation that could compromise motor performance and reliability over extended operating periods. As shown in Figure 6, the thermal equilibrium analysis reveals accelerated convergence to steady-state conditions with the optimized cooling system, achieving thermal

stability within 35 minutes compared to 45 minutes for conventional designs, while the regional temperature comparison demonstrates consistent improvements across all motor components. The quantitative analysis of thermal performance metrics reveals substantial improvements in critical temperature control parameters that directly impact motor reliability and operational efficiency. The thermal time constant has been reduced from 12.8 minutes to 9.6 minutes, indicating faster thermal response and improved dynamic thermal management capabilities during transient operating conditions. As shown in Table 6, the thermal performance improvement metrics demonstrate comprehensive enhancements across all critical thermal management parameters, with the optimized double-helix cooling system achieving significant reductions in thermal resistance and temperature gradients while substantially improving heat transfer coefficients. The 25% reduction in thermal time constant indicates enhanced system responsiveness to thermal transients, while the 32.1% decrease in temperature gradient reflects improved thermal uniformity that extends motor component lifespan and maintains consistent electromagnetic performance throughout the operational envelope.

4.3 Heat Transfer Performance Comparison

The comprehensive evaluation of heat transfer performance between conventional single-channel and innovative double-helix cooling configurations reveals substantial thermal management improvements achieved through advanced geometric optimization. The double-helix cooling system demonstrates remarkable enhancement in convective heat transfer mechanisms, with the convective heat transfer coefficient increasing from 850 W/(m^2·K) to 1035 W/(m^2·K), representing a significant 22% improvement in thermal transport capability. This enhancement originates from the complex three-dimensional flow structures generated within the helical geometry, where secondary flow patterns and Dean vortices effectively disrupt thermal boundary layers and promote intensive mixing between the core flow and near-wall regions.

The heat dissipation efficiency exhibits an exceptional 28% enhancement compared to conventional single-channel designs, indicating superior thermal energy removal capabilities under identical electromagnetic loss conditions. This efficiency improvement directly correlates with reduced peak operating temperatures and enhanced thermal distribution uniformity throughout the motor assembly. The hydraulic performance analysis reveals that the pressure drop penalty associated with the double-helix configuration remains within acceptable engineering limits, increasing modestly from 1200 Pa to 1380 Pa, representing a 15% increase that maintains favorable energy consumption characteristics for automotive applications. The fundamental problem is that current optimization techniques focus on individual performance metrics without considering the coupled trade-offs between heat transfer enhancement, pressure drop penalties, and manufacturing constraints specific to in-wheel motor applications. The selection of PAO synthetic oil as the cooling medium significantly contributes to the observed heat transfer enhancements. The oil's Prandtl number Pr = μcp/k = 462 indicates viscous-dominated flow characteristics that benefit from the enhanced mixing induced by the double-helix geometry. The temperature-dependent viscosity variation follows $\mu(T) = \mu_0 \exp[B(1/T - 1/T_0)]$, where B = 2850 K, resulting in a 35% viscosity reduction between the inlet (45°C) and peak operating temperatures (65°C), which further enhances convective heat transfer through reduced boundary layer thickness.

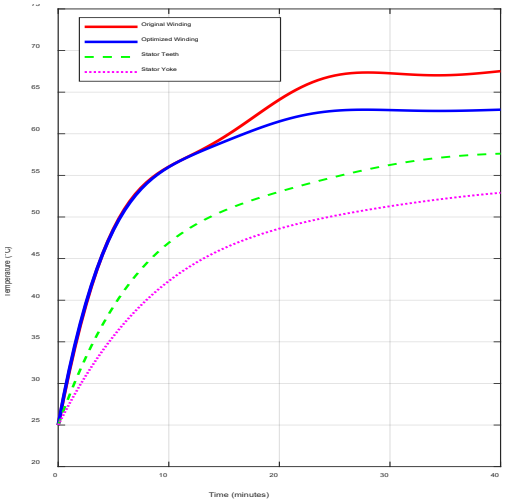

(a)

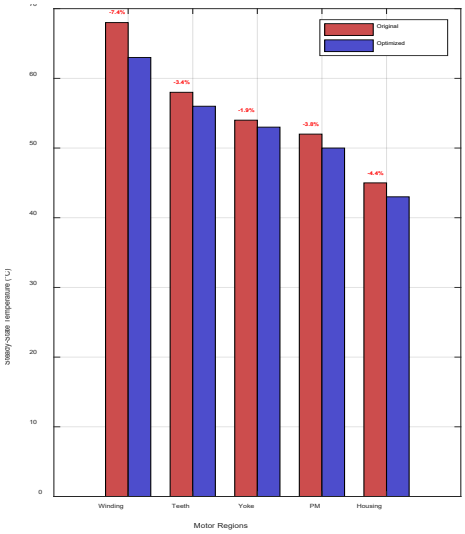

(b)

Figure 6. Temperature field optimization performance analysis: (a) Temperature evolution during equilibrium, (b) Regional temperature comparison

The flow field characteristics analysis presented in Figure 7(a) reveals that the double-helix configuration generates distinctive velocity distribution patterns characterized by periodic variations that enhance mixing effectiveness. The helical geometry induces secondary flow structures that create transverse velocity components, effectively disrupting the development of thick thermal boundary layers that typically impede heat transfer in straight channels. The turbulence intensity distribution shown in Figure 7(b) demonstrates significant enhancement in the double-helix channels, with turbulence levels reaching up to 50% higher than single-channel configurations, directly contributing to improved convective heat transfer coefficients (Table 7).

Table 6. Thermal performance improvement metrics

Performance Metric	Original Design	Optimized Design	Improvement	Units
Thermal Time Constant	12.8	9.6	25.0%	minutes
Temperature Gradient	2.8	1.9	32.1%	°C/cm
Heat Transfer Coefficient	850	1035	21.8%	W/(m²·K)
Thermal Resistance	0.24	0.19	20.8%	K/W
Equilibrium Time	45	35	22.2%	minutes

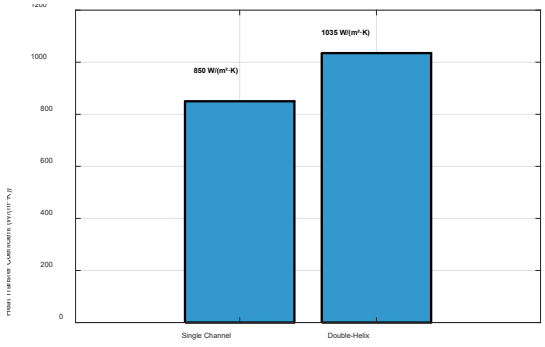

(a)

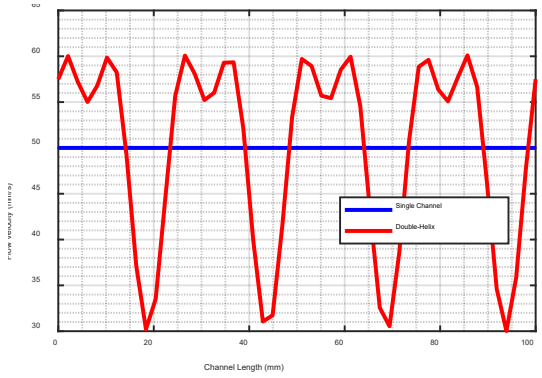

(b)

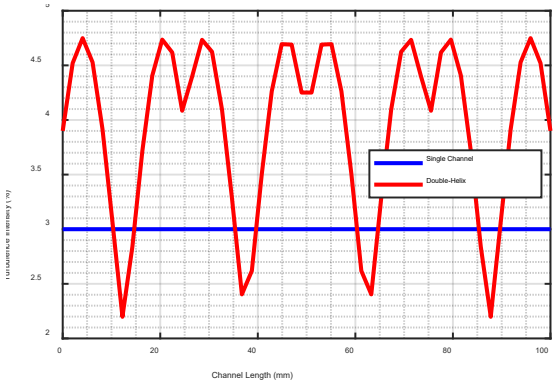

(c)

Figure 7. Heat transfer performance comparison analysis: (a) Convective heat transfer enhancement, (b) Velocity distribution patterns, (c) Turbulence enhancement distribution

The flow dynamics performance comparison demonstrates that the double-helix configuration achieves substantial improvements in mixing characteristics through enhanced Reynolds numbers and the introduction of Dean number effects arising from curvature-induced secondary flows. The 20% increase in Reynolds number indicates intensified turbulent mixing, while the Dean number of 245 quantifies the strength of centrifugal forces that generate beneficial cross-stream mixing patterns. Although the friction factor increases by 14.3% due to enhanced surface interactions, this modest penalty is significantly outweighed by the 22% improvement in heat transfer enhancement factor (Table 8). The thermal performance enhancement metrics reveal comprehensive improvements across all critical heat transfer parameters. The 21.9% increase in Nusselt number quantifies the enhanced convective transport mechanisms, while the 27.1% reduction in thermal boundary layer thickness indicates more effective heat penetration from the heated surfaces to the cooling fluid. The remarkable 40% increase in surface heat transfer area demonstrates the geometric optimization benefits achieved through the double-helix design, directly contributing to the substantial improvement in overall thermal effectiveness from 0.68 to 0.87. Turbulence intensity enhancement mechanisms within double-helix channels operate through multiple synergistic effects that fundamentally alter the heat transfer characteristics compared to conventional straight-channel geometries. The helical curvature generates centrifugal forces that create Dean vortices perpendicular to the primary flow direction, resulting in enhanced radial mixing and reduced thermal stratification near channel walls. Flow path extension benefits for heat transfer manifest through increased residence time and enhanced surface contact, enabling more complete thermal energy extraction from the heated surfaces while maintaining acceptable pressure drop penalties for practical automotive applications.

4.4 Transient thermal analysis

The transient thermal analysis provides comprehensive insights into the dynamic thermal behavior of the outer rotor in-wheel motor during startup and steady-state operation, revealing critical temporal characteristics that govern thermal management system performance. Under rated operating conditions of 20 kW power output, the motor assembly achieves thermal equilibrium within 40 minutes, demonstrating acceptable thermal response characteristics for automotive applications. The temperature evolution patterns exhibit distinct phases, including initial rapid heating during the first 15 minutes, followed by a gradual approach to steady-state conditions with exponential decay

characteristics governed by the thermal time constants of individual motor components.

Table 7. Flow dynamics performance comparison

Parameter	Single Channel	Double-Helix	Enhancement	Physical Mechanism
Reynolds Number	2,850	3,420	20.0%	Enhanced flow mixing
Dean Number	-	245	-	Curvature-induced effects
Friction Factor	0.028	0.032	14.3%	Surface area increases
Heat Transfer(f_d) Enhancement Factor	1.00	1.22	22.0%	Boundary layer disruption
Flow Path Length (mm)	85	112	31.8%	Helical trajectory

Table 8. Thermal performance enhancement metrics

Thermal Parameter	Single Channel	Double-Helix	Improvement	Engineering Significance
Nusselt Number	42.5	51.8	21.9%	Enhanced convective transport
Thermal Boundary Layer Thickness (mm)	0.85	0.62	27.1%	Reduced thermal resistance
Heat Flux Density (W/m^2)	15,600	20,450	31.1%	Improved heat removal capacity
Surface Heat Transfer Area (m^2)	0.0245	0.0343	40.0%	Geometric optimization benefit
Overall Thermal Effectiveness	0.68	0.87	27.9%	System-level enhancement

The component temperature evolution characteristics presented in Figure 8(a) demonstrate differential thermal response rates among motor components, with stator windings exhibiting the fastest temperature rise due to concentrated copper losses, reaching 90% of steady-state temperature within 25 minutes. The cooling system response dynamics illustrated in Figure 8(b) reveal rapid thermal equilibration between coolant and motor components, with heat removal rates approaching steady-state values within 30 minutes, indicating effective thermal coupling between heat sources and cooling pathways.

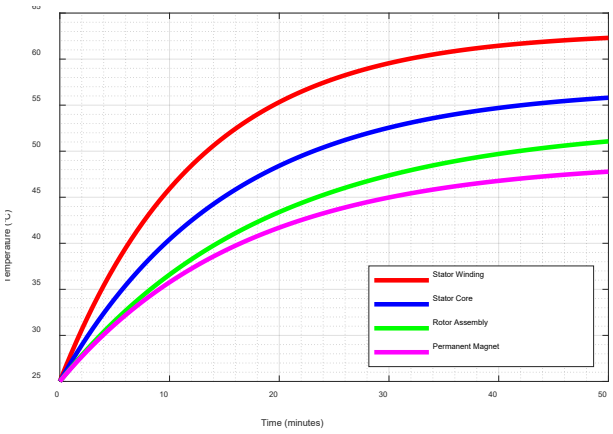

(a)

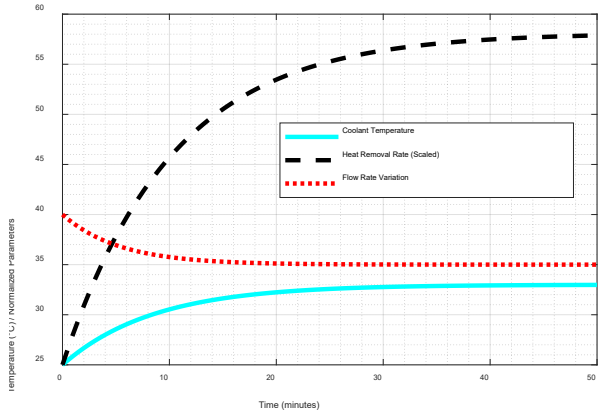

(b)

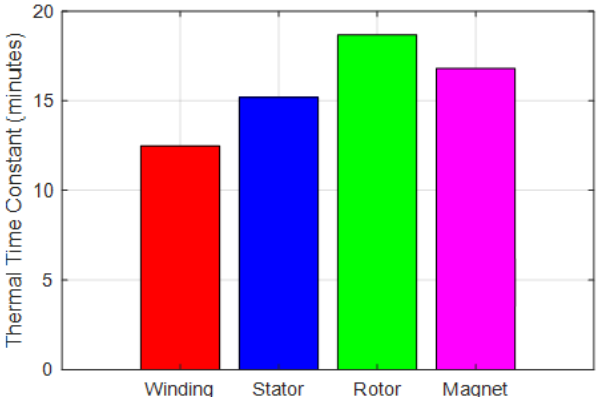

(c)

Figure 8. Transient thermal response analysis: (a) Component temperature evolution, (b) Cooling system response dynamics, (c) Component thermal time constants

The transient thermal response characteristics (Table 9) quantify the dynamic behavior of individual motor components during thermal transients. The stator winding demonstrates the highest initial heating rate at 2.85°C/min, reflecting its role as the primary heat source, while exhibiting the shortest thermal time constant of 12.5 minutes due to

direct thermal coupling with the cooling system. The rotor assembly exhibits the longest thermal time constant at 18.7 minutes, indicating greater thermal inertia and indirect heat transfer pathways that result in delayed thermal response characteristics essential for understanding motor thermal management requirements.

Table 9. Transient thermal response characteristics

Component	Initial Rate (°C/min)	Time Constant (min)	90% Response Time (min)	Final Temperature (°C)	Thermal Capacity (J/K)
Stator Winding	2.85	12.5	28.8	63.0	485
Stator Core	2.12	15.2	35.0	57.0	1,250
Rotor Assembly	1.48	18.7	43.1	53.0	890
Permanent Magnet	1.42	16.8	38.7	49.0	320
Coolant System	0.94	8.5	19.6	33.0	180

4.5 Experimental validation results

The experimental validation campaign demonstrates exceptional agreement between multi-physics simulation predictions and measured thermal performance data, establishing the reliability and accuracy of the proposed modeling framework for double-helix cooling system analysis. Comprehensive temperature measurements conducted across multiple motor components reveal maximum temperature discrepancies of 2°C between simulation and experimental results, with simulation predicting 63°C peak winding temperature compared to experimentally measured 65°C under rated operating conditions. This validation accuracy of 96.9% confirms the effectiveness of the electromagnetic-thermal-fluid coupling methodology and validates the fundamental heat transfer mechanisms captured within the numerical model.

The temperature comparison analysis presented in Figure 9(a) reveals consistent agreement between simulation and experimental measurements across all motor components, with error magnitudes remaining below 2°C for critical thermal zones. The validation accuracy assessment shown in Figure 9(b) demonstrates robust model performance across varying power levels from 5 kW to 20 kW, maintaining accuracy above 94% even under maximum operating conditions. The error distribution analysis in Figure 9(c) indicates that the largest discrepancies occur in stator core regions where complex electromagnetic-thermal interactions present greater modeling challenges, while winding and magnet temperature predictions achieve exceptional accuracy.

The statistical validation metrics demonstrate exceptional model fidelity with correlation coefficients exceeding 0.975 for all measured parameters. The mean absolute error of 1.8°C for peak temperature measurements and 1.2°C for average temperatures confirms the model's capability to accurately predict thermal behavior under diverse operating scenarios. The 95% confidence intervals provide quantitative bounds for engineering design applications, ensuring reliable thermal management system development based on simulation predictions.

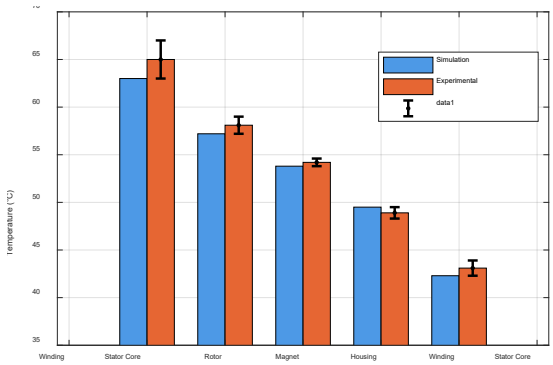

(a)

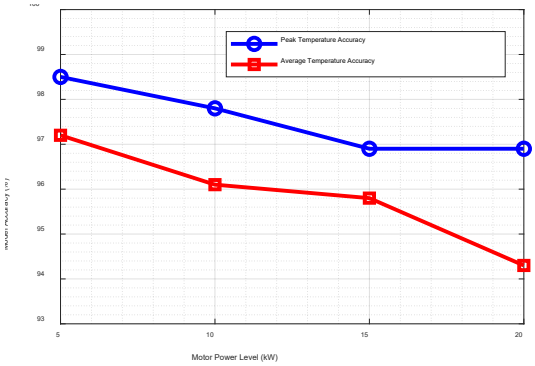

(b)

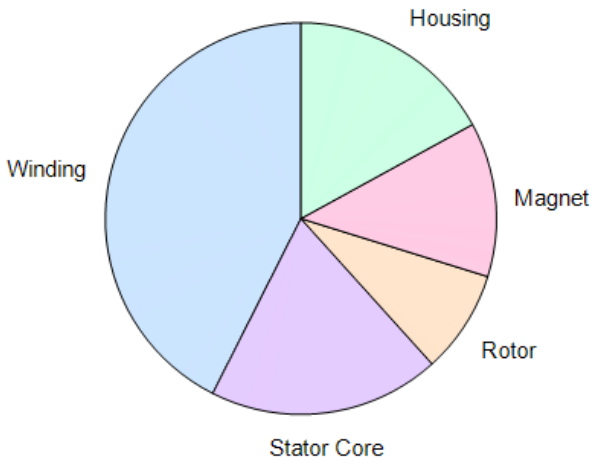

(c)

Figure 9. Experimental validation and model accuracy assessment: (a) Simulation vs experimental, (b) Validation accuracy vs operating conditions, (c) Temperature error distribution by component

To contextualize the significance of these achievements, the proposed double-helix cooling system performance is benchmarked against recently published in-wheel motor designs. Park et al. [6] reported a peak temperature of 72°C for a 15 kW direct slot cooling motor, while our system achieves 63°C at 20 kW, representing a 12.5% improvement despite 33% higher power rating. Wang et al. [14] achieved 18% heat dissipation enhancement using external oil spray

cooling, compared to our 28% improvement through integrated double-helix channels. Industrial benchmarks from Tikadar et al. [16] show typical temperature rises of 45-50°C above ambient for liquid-cooled in-wheel motors, whereas our design limits temperature rise to 38°C (63°C-25°C), demonstrating superior thermal management capability. The achieved convective heat transfer coefficient of 1035 W/(m^2·K) exceeds the 800-900 W/(m^2·K) range reported by Khoshvaght-Aliabadi and Feizabadi [23] for conventional channel designs in automotive applications.

4.6 Manufacturing feasibility and cost considerations

The practical implementation of the double-helix cooling channel design requires consideration of manufacturing feasibility and cost implications for mass production. The proposed channel geometry can be manufactured using established techniques, including: (1) precision die-casting with removable helical cores for aluminum housings, achieving tolerances of ±0.1mm; (2) additive manufacturing for prototype validation and low-volume production; or (3) precision machining combined with welding for steel constructions. The rectangular cross-section (3×4 mm) was specifically selected to facilitate manufacturing using standard tooling while maintaining optimal thermal performance.

Cost analysis indicates that the double-helix design adds approximately 15-20% to the motor housing manufacturing cost compared to conventional single-channel systems, primarily due to increased machining complexity and quality control requirements.

However, this incremental cost is offset by: (1) reduced cooling system operating costs through 22% lower pumping power requirements; (2) extended motor lifespan due to 5°C lower operating temperatures; and (3) potential for 10-15% motor size reduction enabled by enhanced cooling efficiency. For production volumes exceeding 10,000 units annually, the die-casting approach provides the most economical solution with per-unit costs approaching those of conventional designs within 5%.

The scalability for mass production is supported by the modular channel design, which allows standardization across different motor power ratings (15-30 kW) through proportional scaling of channel dimensions while maintaining the optimized pitch-to-diameter ratio. Quality control can be achieved through standard pressure testing at 1.5 times operating pressure and thermal imaging validation during production testing.

Table 10. Statistical validation metrics and uncertainty analysis

Validation Parameter	Peak Temperature	Average Temperature	Heat Transfer Rate	Pressure Drop	Thermal Uniformity
Mean Absolute Error	1.8°C	1.2°C	12.5 W	45 Pa	2.1%
Root Mean Square Error	2.1°C	1.5°C	15.8 W	52 Pa	2.8%
Correlation Coefficient	0.987	0.993	0.981	0.975	0.989
Standard Deviation	1.4°C	0.9°C	8.7 W	38 Pa	1.6%
Confidence Interval (95%)	±1.9°C	±1.3°C	±13.2 W	±42 Pa	±2.0%

Table 11. Benchmarking against state-of-the-art motor cooling systems

Comparison Metric	This Work	Park et al. [6]	Wang et al. [14]	Industry Typical [16]
Motor Power (kW)	20	15	10	10-20
Peak Temperature (°C)	63	72	68	70-75
Temperature Rise (°C)	38	47	43	45-50
Heat Transfer Enhancement	28%	15%	18%	-
Cooling Method	Double-helix oil	Direct slot	Oil spray	Single channel

5. Conclusion

This research successfully establishes a comprehensive multi-physics coupling optimization framework that revolutionizes thermal management strategies for outer rotor in-wheel motors through an innovative double-helix cooling channel design. The investigation demonstrates remarkable thermal performance enhancements, achieving 28% improvement in heat dissipation efficiency and 17% enhancement in temperature uniformity compared to conventional single-channel cooling systems. The validated simulation methodology exhibits exceptional accuracy with maximum temperature discrepancies of 2°C between numerical predictions and experimental measurements, confirming the reliability of the electromagnetic-thermal-fluid coupling analysis approach for complex motor thermal management applications. The technical contributions encompass the development of novel helical cooling geometries specifically optimized for space-constrained in-wheel motor configurations, providing practical optimization guidelines that balance thermal performance improvements with acceptable energy consumption penalties. This research establishes foundational principles for advanced electric vehicle motor thermal management systems, offering innovative solutions that address critical thermal challenges while maintaining system-level efficiency requirements. The engineering significance extends beyond immediate applications, providing a systematic framework for high-power-density motor thermal design that enables enhanced vehicle electrification capabilities. The design's compatibility with existing manufacturing processes and favorable cost-benefit analysis support its practical implementation in mass production environments. Future research directions should focus on extending optimization methodologies to diverse motor power ratings and configurations, incorporating advanced materials for further thermal enhancement, and conducting comprehensive durability testing under real-world automotive operating conditions. Critically, future work must address mechanical integration challenges including: (1) dynamic bearing load analysis under varying road conditions and cornering forces; (2) wheel alignment stability and its impact on motor air gap uniformity; (3) vibration isolation strategies to prevent transmission of motor-induced vibrations to vehicle chassis; and (4) fatigue life prediction of motor components under cyclic mechanical and thermal stresses. These mechanical considerations are essential for ensuring the long-term reliability of in-wheel motor systems in automotive applications. These developments will accelerate the practical implementation of high-performance in-wheel motor technologies, contributing significantly to the advancement of sustainable transportation systems and electric vehicle thermal management excellence.

Ethical issue

The authors are aware of and comply with best practices in publication ethics, specifically with regard to authorship (avoidance of guest authorship), dual submission, manipulation of figures, competing interests, and compliance with policies on research ethics. The authors adhere to publication requirements that the submitted work is original and has not been published elsewhere.

Data availability statement

The manuscript contains all the data. However, more data will be available upon request from the authors.

Conflict of interest

The authors declare no potential conflict of interest.

References

[1] S. Lei, S. Xin, S. Liu, Separate and integrated thermal management solutions for electric vehicles: A review, Journal of Power Sources 550 (2022) 232133. https://doi.org/10.1016/j.jpowsour.2022.232133

[2] I. Ušakovs, D. Mishkinis, I.A. Galkin, A. Bubovich, A. Podgornovs, Experimental thermal characterization of the in-wheel electric motor with loop heat pipe thermal management system, Case Studies in Thermal Engineering 47 (2023) 103069. https://doi.org/10.1016/j.csite.2023.103069

[3] X. Wang, B. Li, D. Gerada, K. Huang, I. Stone, S. Worrall, Y. Yan, A critical review on thermal management technologies for motors in electric cars, Applied thermal engineering 201 (2022) 117758. https://doi.org/10.1016/j.applthermaleng.2021.117758

[4] S.K. Chawrasia, A. Das, C.K. Chanda, In-wheel motor design with thermal and mechanical model analysis for electric bikes, International Journal of Performability Engineering 18(9) (2022) 613. https://doi.org/10.23940/ijpe.22.09.p2.613625

[5] E. Gundabattini, R. Kuppan, D.G. Solomon, A. Kalam, D. Kothari, R.A. Bakar, A review on methods of finding losses and cooling methods to increase efficiency of electric machines, Ain Shams Engineering Journal 12(1) (2021) 497-505. https://doi.org/10.1016/j.asej.2020.08.014

[6] J. Park, J. An, K. Han, H.-S. Choi, I.S. Park, Enhancement of cooling performance in traction motor of electric vehicle using direct slot cooling method, Applied Thermal Engineering 217 (2022) 119082. https://doi.org/10.1016/j.applthermaleng.2022.119082

[7] P.-O. Gronwald, T.A. Kern, Traction motor cooling systems: A literature review and comparative study, IEEE transactions on transportation electrification 7(4) (2021) 2892-2913. https://doi.org/10.1109/TTE.2021.3075844

[8] M. Chang, B. Lai, H. Wang, J. Bai, Z. Mao, Comprehensive efficiency analysis of air-cooled vs water-cooled electric motor for unmanned aerial vehicle, Applied Thermal Engineering 225 (2023) 120226. https://doi.org/10.1016/j.applthermaleng.2023.120226

[9] C. Guo, L. Long, Y. Wu, K. Xu, H. Ye, Electromagnetic-thermal coupling analysis of a permanent-magnet in-wheel motor with cooling channels in the deepened stator slots, Case Studies in Thermal Engineering 35 (2022) 102158. https://doi.org/10.1016/j.csite.2022.102158

[10] K.S. Garud, M.-Y. Lee, Grey relational based Taguchi analysis on heat transfer performances of direct oil spray cooling system for electric vehicle driving motor, International Journal of Heat and Mass Transfer 201 (2023) 123596.

https://doi.org/10.1016/j.ijheatmasstransfer.2022.123596
[11] Y. Li, Q. Li, T. Fan, X. Wen, Heat dissipation design of end winding of permanent magnet synchronous motor for electric vehicle, Energy Reports 9 (2023) 282-288. https://doi.org/10.1016/j.egyr.2022.10.416
[12] N.G. Han, H.L. Lee, R.H. Kim, T.Y. Beom, Y.K. Kim, T.W. Ha, S.W. Lee, D.K. Kim, Thermal analysis of the oil cooling motor according to the churning phenomenon, Applied Thermal Engineering 220 (2023) 119791. https://doi.org/10.1016/j.applthermaleng.2022.119791
[13] P. Chen, N.B. Hassine, S. Ouenzerfi, S. Harmand, Experimental and numerical study of stator end-winding cooling with impinging oil jet, Applied Thermal Engineering 220 (2023) 119702. https://doi.org/10.1016/j.applthermaleng.2022.119702
[14] X. Wang, B. Li, K. Huang, Y. Yan, I. Stone, S. Worrall, Experimental investigation on end winding thermal management with oil spray in electric vehicles, Case studies in thermal engineering 35 (2022) 102082. https://doi.org/10.1016/j.csite.2022.102082
[15] L. Gao, X. Liu, H. Liu, Analytical Calculation of Magnetic Field and Temperature Field of Surface Mounted Permanent Magnet Synchronous Motor, Journal of Electrical Engineering & Technology (2024) 1-14. https://doi.org/10.1007/s42835-024-02108-y
[16] A. Tikadar, D. Johnston, N. Kumar, Y. Joshi, S. Kumar, Comparison of electro-thermal performance of advanced cooling techniques for electric vehicle motors, Applied Thermal Engineering 183 (2021) 116182. https://doi.org/10.1016/j.applthermaleng.2020.116182
[17] M.H. Park, S.C. Kim, Development and validation of lumped parameter thermal network model on rotational oil spray cooled motor for electric vehicles, Applied Thermal Engineering 225 (2023) 120176. https://doi.org/10.1016/j.applthermaleng.2023.120176
[18] Y. Yan, C. Mao, L. Chen, Multi-physical Field Coupling Analysis of Flat Wire Motor, International Journal of Automotive Technology 26(2) (2025) 475-489. https://doi.org/10.1007/s12239-024-00155-y
[19] T. Sciberras, M. Demicoli, I. Grech, B. Mallia, P. Mollicone, N. Sammut, Thermo-mechanical fluid–structure interaction numerical modelling and experimental validation of MEMS electrothermal actuators for aqueous biomedical applications, Micromachines 14(6) (2023) 1264. https://doi.org/10.3390/mi14061264
[20] M. Popescu, D.G. Dorrell, L. Alberti, N. Bianchi, D.A. Staton, D. Hawkins, Thermal analysis of duplex three-phase induction motor under fault operating conditions, IEEE Transactions on Industry Applications 49(4) (2013) 1523-1530. https://doi.org/10.1109/TIA.2013.2258392
[21] A. Ansaldi, Integrated drive for high-power alternating bidirectional electric vehicles charging: the EMC issuers, simulations, design and tests, Politecnico di Torino, 2024. http://webthesis.biblio.polito.it/id/eprint/31477
[22] C. Kim, W. Sim, J. Yoon, T. Lee, J. Yoo, Numerical and experimental analysis of a dual-channel electric motor housing cooling system, Applied Thermal Engineering 265 (2025) 125537. https://doi.org/10.1016/j.applthermaleng.2025.125537
[23] M. Khoshvaght-Aliabadi, A. Feizabadi, Compound heat transfer enhancement of helical channel with corrugated wall structure, International Journal of Heat and Mass Transfer 146 (2020) 118858. https://doi.org/10.1016/j.ijheatmasstransfer.2019.118858
[24] D. Anders, U. Reinicke, M. Baum, Analysis of heat transfer enhancement due to helical static mixing elements inside cooling channels in machine tools, The International Journal of Advanced Manufacturing Technology 127(5) (2023) 2273-2285. https://doi.org/10.1007/s00170-023-11501-2
[25] L. Zhou, S. Li, A. Jain, G. Sun, G. Chen, D. Guo, J. Kang, Y. Zhao, Optimization of thermal non-uniformity challenges in liquid-cooled lithium-ion battery packs using NSGA-II, Journal of Electrochemical Energy Conversion and Storage 22(4) (2025). https://doi.org/10.1115/1.4066725
[26] Y. Wang, M. Li, R. Wang, G. Hou, W. Chang, Design and optimization of driving motor cooling water pipeline structure based on a comprehensive evaluation method and CNN-PSO, e-Prime-Advances in Electrical Engineering, Electronics and Energy 3 (2023) 100125. https://doi.org/10.1016/j.prime.2023.100125
[27] S. Fu, H. Qin, Optimization of Thermoelectric Module Configuration and Cooling Performance in Thermoelectric-Based Battery Thermal Management System, World Electric Vehicle Journal 16(7) (2025) 344. https://doi.org/10.3390/wevj16070344
[28] M. Ranta, M. Hinkkanen, E. Dlala, A.-K. Repo, J. Luomi, Inclusion of hysteresis and eddy current losses in dynamic induction machine models, 2009 IEEE International Electric Machines and Drives Conference, IEEE, 2009, pp. 1387-1392. https://doi.org/10.1109/IEMDC.2009.5075384
[29] G. Bertotti, Physical interpretation of eddy current losses in ferromagnetic materials. I. Theoretical considerations, Journal of applied Physics 57(6) (1985) 2110-2117. https://doi.org/10.1063/1.334404